Journal of Controlled Release 235 (2016) 236–244

Contents lists available at ScienceDirect

Journal of Controlled Release

journal homepage: www.elsevier.com/locate/jconrel

Influence of particle size on the *in vivo* potency of lipid nanoparticle formulations of siRNA

Sam Chen [a], Yuen Yi C. Tam [a], Paulo J.C. Lin [a,b], Molly M.H. Sung [a], Ying K. Tam [a,b], Pieter R. Cullis [a,*]

[a] Department of Biochemistry and Molecular Biology, University of British Columbia, 2350 Health Sciences Mall, Vancouver, British Columbia V6T 1Z3, Canada
[b] Acuitas Therapeutics, 2714 West 31st Avenue, Vancouver, British Columbia V6L 2A1, Canada

ARTICLE INFO

Article history:
Received 13 November 2015
Received in revised form 15 May 2016
Accepted 25 May 2016
Available online 26 May 2016

Keywords:
Lipid nanoparticles
Liposomes
siRNA
Nanomedicine
Drug delivery
Lipid exchange

ABSTRACT

Lipid nanoparticles (LNP) can provide a clinically effective method for delivering small interfering RNA (siRNA) to silence pathological genes in hepatocytes. The gene silencing potency of these LNP-siRNA systems has been shown to depend on a variety of factors including association with serum factors such as ApoE and the pK_a of component ionizable lipids. Here we investigate the influence of LNP size, an important parameter affecting tissue penetration of LNP systems, on the pharmacokinetics, biodistribution, and hepatic gene silencing potency of LNP-siRNA systems following intravenous administration. For LNP systems stabilized by a polyethylene glycol (PEG)-lipid that can dissociate from the LNP following injection, it is shown that small (diameter ≤ 30 nm) systems are considerably less potent than their larger counterparts. This is attributed in part to the ability of other lipid components, particularly the ionizable amino-lipid, to dissociate from the LNP following dissociation of the PEG-lipid. Small LNP stabilized by PEG-lipids with slow dissociation rates exhibited much reduced amino-lipid dissociation rates, however such systems are relatively impotent due to the continued presence of the PEG coating. These results demonstrate the delicate balance between the *in vivo* potency of LNP-siRNA systems and the residence times of component lipids in the LNP particle itself and suggest new directions to optimize the *in vivo* gene silencing potency of small LNP-siRNA systems.

1. Introduction

The therapeutic potential of siRNA is considerable given its ability to block the production of disease-associated gene products, including proteins considered "undruggable" by conventional approaches [1]. However, challenges for the therapeutic use of "naked" siRNA include breakdown in biological fluids, limited distribution to target tissues and the relative inability of these macromolecules to cross target cell membranes [2,3]. This has stimulated development of many technologies to deliver siRNA. Lipid nanoparticle (LNP) systems are the most clinically advanced siRNA delivery systems [4] and are in clinical trials for the treatment of hypercholesterolemia, transthyretin–mediated amyloidosis and liver cancer [5–7].

Previous work has shown that the *in vivo* potency of LNP-siRNA systems for hepatic gene silencing depends strongly on the ionizable amino-lipid contained in the LNP. This earlier work was stimulated by the reasoning that the cationic lipid should engender maximum bilayer destabilizing capacity on interacting with endogenous anionic lipids at endosomal pH values but should be relatively neutral at physiological pH values to avoid rapid clearance and toxicity concerns [8,9]. This approach has led to the identification of dilinoleylmethyl-4-dimethylaminobutyrate (DLin-MC3-DMA) as the current gold standard amino-lipid for efficient gene silencing in hepatocytes *in vivo* following intravenous (i.v.) administration. LNP containing DLin-MC3-DMA have achieved 50% gene silencing at doses as low as 0.005 mg siRNA/kg in mice and 0.03 mg siRNA/kg in non-human primates after a single i.v. injection [9].

Optimization of other components of LNP-siRNA delivery systems has received less attention. It has been shown that the constituent polyethylene glycol (PEG)-lipid is an important component of the LNP in that the presence of a PEG coating inhibits cell uptake and thus reduces potency [10,11]. This has led to the use of PEG-lipids with short (C_{14}) acyl chains that are able to rapidly exchange out of LNP following administration [12]. More recently it has been shown that by increasing the proportion of the PEG-lipid in the initial formulation, LNP as small as 20 nm in diameter can be generated employing microfluidic mixing techniques [13–15]. In this regard there are compelling reasons for developing potent LNP-siRNA systems that are as small as possible to enable translocation from the lung to the lymph nodes [16], drainage into the lymphatic system [17,18], and infiltration into poorly vascularized tumors [19–21]. For example, we have shown that small 30 nm diameter LNP are better able to drain to local lymph nodes and

* Corresponding Author at: 2350 Health Sciences Mall, Vancouver, British Columbia V6T 1Z3,Canada.
E-mail address: pieterc@mail.ubc.ca (P.R. Cullis).

http://dx.doi.org/10.1016/j.jconrel.2016.05.059
0168-3659/

enter the peripheral circulation after subcutaneous (s.c.) administration [15]. However, these LNP-siRNA systems were less potent agents for hepatic gene silencing than their larger 45 nm diameter counterparts.

In this work we continue efforts to develop small LNP-siRNA systems that are highly potent. In order to remove confounding effects due to s.c. administration and the attendant need to drain from the site of injection, hepatic gene silencing was characterized following i.v administration. It is shown that the decreased potency of small 30 nm LNP-siRNA systems can be attributed, at least in part, to a pronounced instability of LNP-siRNA systems as their size is reduced below 45 nm diameter.

2. Materials and methods

2.1. Materials

1,2-distearoyl-sn-glycero-3-phosphocholine (DSPC) was purchased from Avanti Polar Lipids (Alabaster, AL) and cholesterol was purchased from Sigma-Aldrich (St. Louis, MO). 3-(dimethylamino)propyl(12Z,15Z)-3-[(9Z,12Z)-octadeca-9,12-dien-1-yl]henicosa-12,15-dienoate (DMAP-BLP), (R)-2,3-bis(octadecyloxy)propyl-1-(methoxy polyethylene glycol 2000) carbamate (PEG-DMG) and (R)-2,3-bis(stearyloxy)propyl-1-(methoxy poly(ethylene glycol)2000 carbamate (PEG-DSG) were synthesized by Alnylam Pharmaceuticals [22,23]. All siRNA were either provided by Alnylam Pharmaceuticals or purchased from Integrated DNA Technologies (San Diego, CA). The siFVII sense and antisense strand sequences are 5′-GGAucAucucAAGucuuAcTT-3′ and 5′-GuAAGAcuuGAGAuGAuccTT-3, respectively, with 2′-Fluoro-modified nucleotides represented in lower case [15,23].

2.2. Preparation of lipid nanoparticle-siRNA systems

LNP-siRNA were prepared by microfluidic mixing as described previously [14,15]. Briefly, DMAP-BLP, DSPC, cholesterol and PEG-lipid were dissolved in ethanol at mole ratios of 50:10:39.5:0.5, respectively. The proportion of PEG-lipid was increased up to 5 mol% at the expense of cholesterol. The lipid in ethanol solution and siRNA prepared in 25 mM acetate buffer (pH 4.0) was then injected into microfluidic mixers (Precision Nanosystems, Vancouver, BC) at a flow rate ratio of 1:3 respectively with a combined final flow rate of 4 mL/min and a siRNA:lipid ratio of 0.056 mg/μmol. Formulations were then dialyzed (Spectrum Labs, Rancho Dominguez, CA) against 50 mM MES and 50 mM citrate buffer (pH 6.7) for at least 4 h followed by phosphate buffered saline (pH 7.4) overnight. In experiments requiring radiolabelled LNP, ^{3}H-cholesteryl hexadecylether (^{3}H-CHE) (Perkin Elmer; Boston, Massachusetts) was incorporated at the ratio of 3.9 μCi/μmol total lipid.

2.3. Analysis of lipid nanoparticles

LNP size (number weighting) was determined by dynamic light scattering using the Malvern Zetasizer NanoZS (Worcestershire, UK). siRNA encapsulation efficiency was determined using the Quant-iT Ribogreen RNA assay (Life Technologies, Burlington, ON). Briefly, LNP-siRNA systems were incubated at 37 °C for 10 min in the presence or absence of 1% Triton X-100 (Sigma-Aldrich, St. Louis, MO). Upon the addition of the Ribogreen reagent, fluorescence intensities (Ex/Em: 480/520 nm) for untreated samples (representing unencapsulated siRNA) and samples treated with Triton X-100 (representing total siRNA) were determined. Total lipid was determined by measuring the cholesterol content using the Cholesterol E assay (Wako Chemicals, Richmond, VA) and the siRNA concentration was determined by measuring the absorbance at 260 nm. Apparent acid dissociation constants (pKa) of LNP-siRNA systems were determined as previously described [9]. Briefly, 2-(p-toluidino)-6-napthalene sulfonic acid (TNS, Sigma-Aldrich, St. Louis, MO) and LNP-siRNA were diluted in pH 2.5–11 buffer containing 10 mM HEPES, 10 mM MES and 10 mM ammonium acetate to a final concentration of 6 μM TNS and 6 μM total lipid. Samples were mixed and fluorescence intensity was measured (Ex/Em: 321/445 nm) using a Perkin Elmer LS55. A sigmoidal best fit analysis was applied and the pKa was measured as the pH at half-maximal fluorescence intensity.

2.4. In vitro lipid and siRNA dissociation

LNP were prepared with 0.5 mol% of ^{14}C labelled DSPC (American Radiolabeled Chemicals, Saint Louis, MO) and 0.25 mol% of ^{3}H labelled PEG-DMG (Alnylam Pharmaceuticals, Cambridge, MA) or 0.5 mol% of ^{14}C labelled dilinoleylmethyl-4-dimethylaminobutyrate (DLin-MC3-DMA, Alnylam Pharmaceuticals) and 0.002 mol% of ^{3}H-CHE. The ^{3}H:^{14}C ratios were maintained at approximately 3:1. For siRNA dissociation studies, siRNA conjugated to Quasar 570 fluorophore (Alnylam Pharmaceuticals) was used. LNP were incubated for 0, 0.25, 1, 2, 4 and 8 h at 37 °C in 200 μL of sterile mouse plasma (Cedarlane, Burlington, Ontario) at a final lipid concentration of 0.3 mM. At the various timepoints, samples were loaded onto a 1.5 × 27 cm Sepharose CL-4B column (Sigma-Aldrich, St. Louis, MO). 30 × 2 mL fractions were collected and analyzed by liquid scintillation counting. To determine the amount of siRNA remaining in the LNP fractions, 135 μL of each fraction was incubated with 0.5 mM hexaethylene glycol monodecyl ether (Sigma-Aldrich, St. Louis, MO) and the fluorescence at 590 nm was measured. All dissociation rates were estimated from a linear fit of the first four timepoints. For experiments monitoring Forster Resonance Energy Transfer (FRET) as a measure of particle stability, LNP were prepared as described previously with the addition of 1 mol% each of 1,2-dioleoyl-sn-glycero-3-phosphoethanolamine-*N*-(7-nitro-2-1,3-benzoxadiazol-4-yl) (NBD-DOPE) and 1,2-dioleoyl-*sn*-glycero-3-phosphoethanolamine-*N*-(lissamine rhodamine B sulfonyl) (LRB-DOPE). LNP were incubated at 37 °C in mouse plasma for up to 24 h at a final lipid concentration of 0.3 mM. Fluorescence of NBD-DOPE was measured (Ex/Em: 485/530 nm) in the presence or absence of 1.5% Triton X-100.

2.5. Pharmacokinetic and biodistribution studies

Female CD1 mice (Charles River Laboratories, Wilmington, MA) were injected with ^{3}H-CHE labelled LNP and euthanized at 15 min, 30 min, 2 h, 7 h and 24 h post-injection and tissues were collected. To determine LNP concentration in each tissue, approximately 600 mg of tissue was homogenized using the FastPrep homogenizer from MP Biomedicals (Santa Ana, CA). Homogenates were incubated with 0.5 mL of Solvable (Perkin Elmer) at 50 °C overnight. Samples were cooled then decolourized with the addition of 200 μL of 30% (v/v) hydrogen peroxide followed by the addition of 5 mL of Pico-Fluor Plus scintillation fluid (Perkin Elmer). To determine LNP concentration in blood, 100 μL of whole blood was added directly to solvable and hydrogen peroxide and allowed to decolourize overnight before the addition of Pico-Fluor Plus. Samples were read on a Beckman LS 6500 liquid scintillation counter.

2.6. In vivo LNP-siRNA activity in the mouse factor VII model

LNP-siRNA were diluted with PBS to the appropriate volume and administered intravenously in 6–8 weeks old female C57Bl/6 mice (Charles River Laboratories, Wilmington, MA). Animals were euthanized after 24 h and blood was collected *via* intracardiac sampling. Serum was separated from whole blood using Microtainer Serum Seperator tubes (Becton Dickinson, Franklin Lakes, NJ) and the residual serum FVII levels were determined using the Biophen VII chromogenic assay (Aniara, Mason, OH) according to manufacturer's protocol and normalized to that of control mice injected with PBS. The doses required to achieve 50% gene silencing (ED_{50}) and the corresponding standard errors (s.e.) were calculated using logarithmic regression analyses on

SigmaPlot 12. All procedures were approved by the Animal Care Committee at the University of British Columbia and were performed in accordance with guidelines established by the Canadian Council on Animal Care.

3. Results

3.1. LNP-siRNA systems with diameter ~80 nm exhibit maximum hepatic gene silencing following i.v. injection

We previously reported that LNP-siRNA with a diameter of ~45–50 nm exhibited most potent hepatic gene silencing following s.c. administration [15]. However, the influence of size on LNP potency in the s.c. model is complicated by the need to drain from the site of injection into the circulation, which favours smaller systems. We therefore examined the influence of LNP size on hepatic gene silencing following i.v. injection, the most direct route of administration. LNP-siRNA systems were produced with different diameters (27 to 117 nm) by varying the PEG-DMG content from 0.25 to 5 mol% lipid. The siRNA was designed to silence coagulation factor VII (siFVII), which is expressed in and secreted by hepatocytes [8,23].

Mice were injected i.v. over the dose range of 0.01 to 3 mg siRNA/kg and FVII levels in blood were determined 24 h post-injection. As shown in Fig. 1A the 78 nm LNP systems exhibited the maximum gene silencing potency. A plot of the siRNA dose required to achieve 50% gene silencing (ED_{50}) *versus* particle size shows that both the smallest (27 nm) and the largest (117 nm) systems were relatively impotent (Fig. 1B). The poor activity of the 117 nm LNP is likely due to an inability to penetrate the fenestrations in the liver vasculature, which are approximately 100–140 nm in diameter in mice [24,25]. However, the lack of potency of the 27 nm diameter LNP (ED_{50} of 0.8 mg/kg), which are 20 times less potent than the 78 nm diameter LNP (ED_{50} of 0.04 mg/kg), cannot be so readily rationalized. For clarity, particle diameters are rounded to the nearest multiple of five herein.

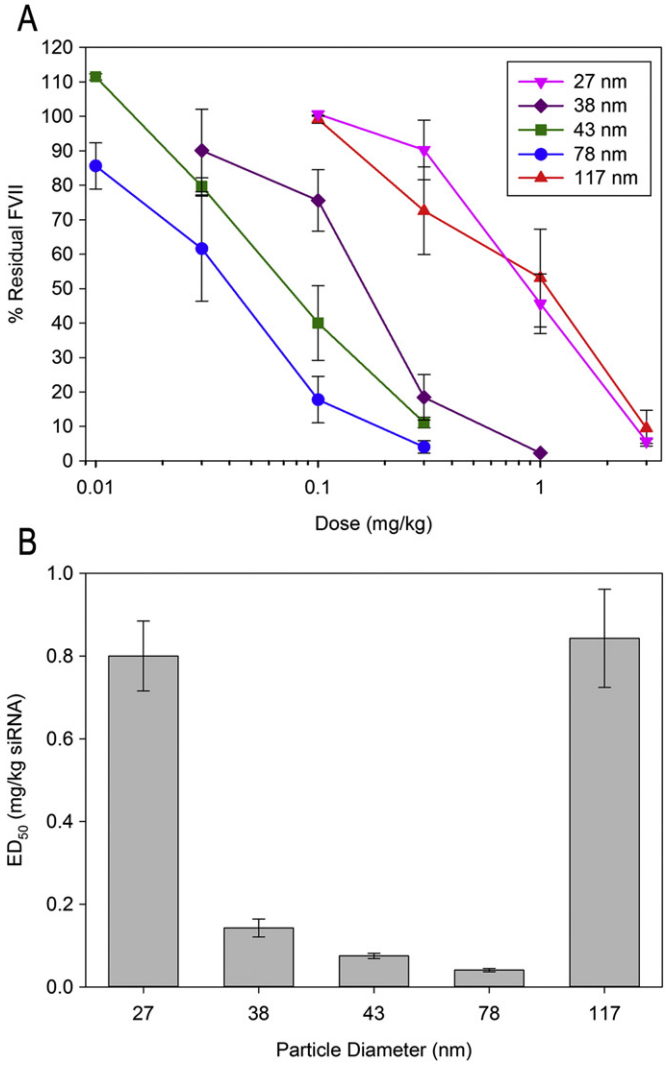

Fig. 1. Hepatocyte gene silencing following i.v. injection of LNP-siRNA systems is dependent on LNP size. LNP-siFVII of various sizes were made by titrating the amount of PEG-DMG lipid present during the formulation process. (A) FVII gene silencing of LNP containing 0.25%, 0.5%, 1.5%, 2.5% or 5% PEG-DMG lipid which resulted in LNP with diameters ranging from 117 to 27 nm. Blood was collected at 24 h post-injection of LNP and FVII levels were determined and normalized to that of control mice injected with PBS. Results shown represent the mean ± s.d. of three animals. (B) The dose required to achieve 50% reduction (ED_{50}) of factor VII protein expression for LNP with different diameters. ED_{50} ± s.e. are calculated from the dose titration curve presented in Fig. 1A.

3.2. LNP of different sizes all distribute rapidly to the liver following i.v. administration

The size-dependent differences in LNP-siRNA activity could result from changes in *in vivo* characteristics such as pharmacokinetics (PK) and biodistribution (BD). To investigate the PK/BD of small (~30 nm diameter), medium (~45 nm diameter) and large (~80 nm diameter) LNPs, trace amounts of ^{3}H-CHE were incorporated into the LNP formulations and concentrations in various tissues were tracked over 24 h in mice post i.v. administration. ^{3}H-CHE was used as a marker for LNP as it has been shown to be non-exchangeable and non-metabolizable [26,27]. As shown in Fig. 2, the 30 nm and 45 nm LNP were very rapidly cleared from the blood compartment with a circulation half-life of <15 min, whereas the larger 80 nm LNP were longer lived with a half-life of ~1.2 h (Fig. 2A). At 24 h post-injection, the vast majority of the LNP were found in the liver, regardless of size (Fig. 2 B and C). Accumulation of LNP in the spleen, kidney, pancreas, lung, femur and heart was also examined. Less than 1% of any formulation was found in these tissues, with the exception of the spleen in which 10% of the 80 nm LNP was found at 24 h (Fig. 2C).

3.3. The stability of LNP-siRNA systems is size dependent

Given the fact that liver accumulation is not dramatically affected by LNP size and therefore is not likely to account for the difference in activity between 30 nm and larger systems, the question is what other effects could be reducing the potency of the smaller systems. Smaller nanoparticles exhibit larger surface to volume ratios with the attendant possibility of increased dissociation rates of LNP components [28,29]. In order to examine the dissociation rates of the PEG-DMG, DSPC, amino-lipid and siRNA, radiolabelled versions of these compounds were obtained and studies were performed to ascertain the ability of these components to exchange out of LNP-siRNA systems when incubated with mouse plasma. It was found that larger LNP-siRNA systems (45 and 80 nm diameter) could be separated from serum components using a Sepharose CL-4B size exclusion column (data not shown). Unfortunately this technique could not be applied to smaller (30 nm diameter) systems because the LNP eluted in the same fraction as lipoproteins in the mouse plasma.

LNP-siRNA systems of 45 and 80 nm diameter were formulated with radiolabelled lipids and were incubated with mouse plasma at 37 °C for up to 8 h and then separated from plasma using size exclusion chromatography as described in Methods. As shown in Fig. 3A, the ^{3}H-CHE remained in the LNP fractions for at least 8 h for both LNP systems. This is expected for this non-exchangeable marker [27]. PEG-DMG is designed to dissociate from LNP systems [8,10] to render them transfection competent, however, as shown in Fig. 3B, the ^{3}H-PEG-DMG in the 45 nm diameter LNP dissociated at a significantly faster rate than for the 80 nm diameter LNP. The halftime ($t_{1/2}$) of dissociation for PEG-

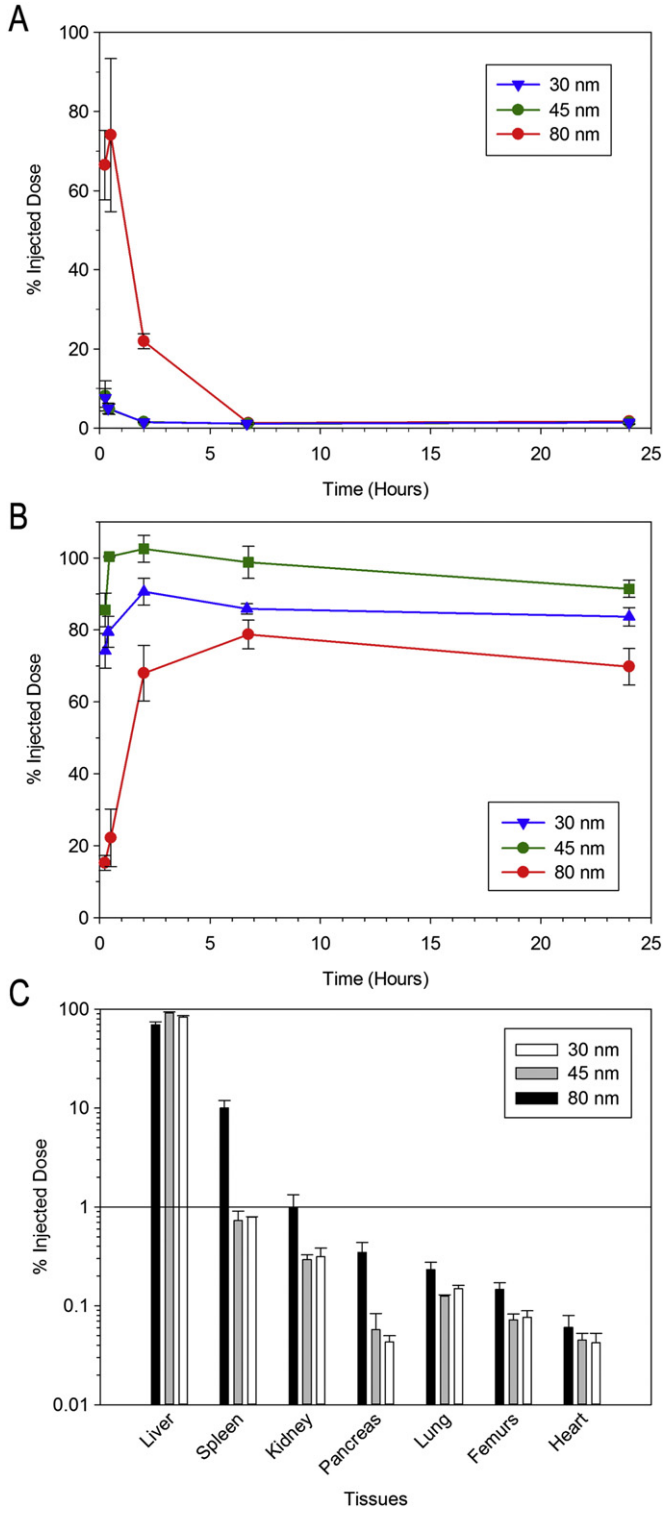

Fig. 2. Circulation lifetime and biodistribution of small, medium and large LNP. Small (30 nm diameter), medium (45 nm diameter) or large (80 nm diameter) LNP labelled with trace amounts of ^{3}H-CHE were injected into mice at 0.3 mg siRNA/kg body weight. Blood and tissues were collected at indicated time points and ^{3}H-CHE levels were determined using liquid scintillation counting. (A) Clearance of LNP from blood over 24 h post i.v. injection. (B) Accumulation of LNP in liver over 24 h post injection. C) Accumulation of LNP in various tissues at 24 h post injection. Results shown represent the mean ± s.d. of four animals.

DMG from the 45 nm diameter LNP can be estimated to be 1.1 h, as compared to 1.7 h for the 80 nm LNP. Furthermore, even the DSPC dissociates from the 45 nm diameter LNP at an appreciable rate ($t_{1/2}$ = 6.2 h) as compared to 80 nm LNP ($t_{1/2}$ = 43 h) (Fig. 3C).

In order to monitor the dissociation of the ionizable amino-lipid, ^{14}C-labelled DLin-MC3-DMA was used as a surrogate for DMAP-BLP. DLin-MC3-DMA is structurally very similar to DMAP-BLP (see Supplementary Fig. 1) and results in similar particle parameters and *in vivo* FVII silencing activity when incorporated into LNP-siRNA systems [9,22]. As shown in Fig. 3D DLin-MC3-DMA dissociated over two times faster from the 45 nm LNP ($t_{1/2}$ = 4.9 h) than from the larger 80 nm system ($t_{1/2}$ = 12 h) (Fig. 3D). It is interesting to note the relatively little loss of the siRNA cargo on plasma incubation for either the 45 or 80 nm diameter LNP systems. There is an initial loss of approximately 20%, possibly corresponding to siRNA adsorbed to the LNP surface, however the remainder of the siRNA cargo remained associated with the LNP for up to 8 h regardless of the initial particle size (Fig. 3E).

The ability of the DSPC and particularly the amino-lipid to dissociate more rapidly from the 45 nm diameter LNP than from the 80 nm diameter system suggests that the relatively poor transfection potency of the 30 nm LNP system could arise from rapid dissociation of the amino-lipid from these systems following *in vivo* administration. In order to corroborate the observation that smaller LNP sizes lead to increased desorption rates of component lipids, a fluorescence resonance energy transfer (FRET)-based assay using NBD-DOPE and LRB-DOPE was developed (Fig. 3F). When these two lipid species are in close proximity, the fluorescence of NBD is quenched by LRB. Thus when NBD or LRB dissociate from the LNP, the NBD fluorescence will recover and can be used to assay for the dissociation of (fluorescent) lipids from the LNP. The relative dissociation rates of these fluorescent lipids should be influenced by particle size in a similar way as other lipid components. LNP-siRNA systems of 30, 45 and 80 nm diameter containing NBD and LRB were incubated with mouse plasma and the NBD fluorescence recovery was measured at 530 nm over 24 h. It was found (Fig. 3F) that NBD and/or LRB dissociated more slowly from the 80 nm LNP (NBD fluorescence recovery $t_{1/2}$ = 4.9 h) than from the 45 nm LNP (NBD fluorescence $t_{1/2}$ = 3.4 h) which was in turn slower than that observed for the 30 nm LNP (fluorescent recovery $t_{1/2}$ = 2.9 h). This observation is consistent with the chromatography-based lipid exchange studies showing that lipids dissociated more slowly from the 80 nm LNP than the 45 nm diameter LNP and suggests that lipids dissociate from the 30 nm LNP even more rapidly.

3.4. Increasing ionizable amino-lipid content improves small LNP-siRNA activity

The lipid dissociation studies suggest that a possible reason for the low potency of the small 30 nm LNP-siRNA systems is that a significant amount of the amino-lipid dissociates from the particle before it reaches or enters the target hepatocytes. The amino-lipid is critical for endosomal destabilization and release of siRNA into the cytoplasm [8,9,30]. If reduced levels of amino-lipid are causing the low potency of the small (30 nm diameter) systems, then higher initial proportions of amino-lipid in the LNP should improve potency. The amine-to-phosphate charge ratio (positive charge on the ionized amino-lipid to the negative charge on the phosphates found on the siRNA), was therefore increased by decreasing the amount of siRNA encapsulated in the LNP and the *in vivo* potency was determined using the FVII assay. When the amine-to-phosphate ratio was increased from 1 to 12 in the 30 nm PEG-DMG LNP-siRNA, a progressive improvement in potency as indicated by the ED_{50} value was observed up to an amine-to-phosphate ratio of 6, with little improvement in LNP activity beyond this point (Fig. 4A). This suggests that a critical amount of excess amino-lipid is necessary for maximum endosome destabilization and that beyond this amount there is little additional benefit.

The amount of amino-lipid was also increased by increasing the molar fraction in the LNP formulation. Previous work has shown that 50 mol% amino-lipid provides optimum activity for systems of 50 nm or greater in diameter [9]. By increasing the amine-to-phosphate ratio from 3 to 6 and increasing the mole fraction of DMAP-BLP in the LNP

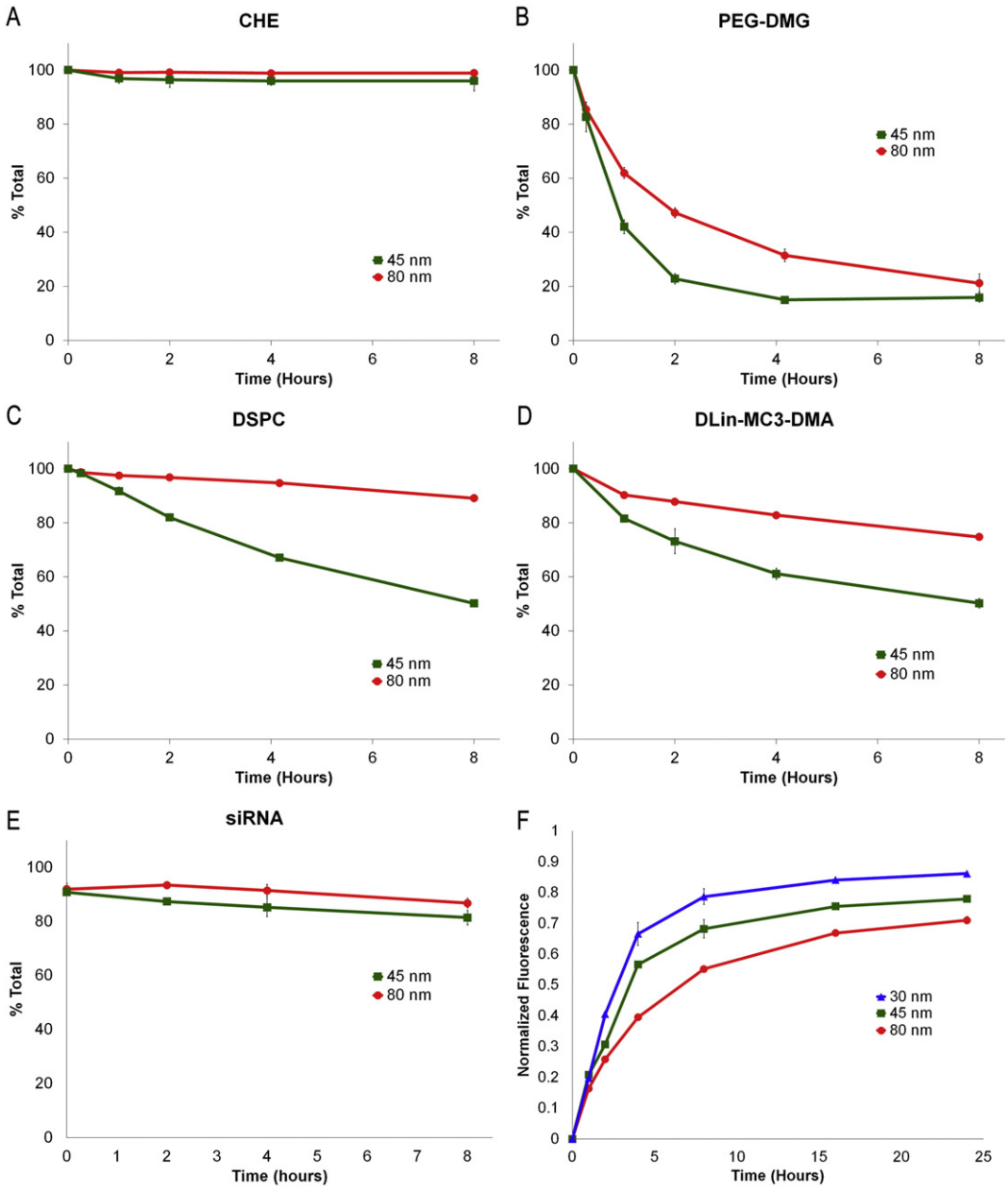

Fig. 3. The rate at which component lipids dissociate from LNP is a sensitive function of LNP size. ^{3}H-PEG-DMG, ^{14}C-DSPC LNP, ^{14}C-DLin-MC3-DMA or ^{3}H-CHE were formulated with either 0.5 mol% or 1.5 mol% PEG-DMG to produce 80 nm or 45 nm diameter LNP and were incubated for 0, 0.25, 1, 2, 4 and 8 h at 37 °C in mouse plasma and separated by size exclusion chromatography. The amounts of each lipid species that remained associated with the LNP fractions were determined over time and the rates of dissociation were determined by fitting to the first four time-points (A-E). (A) The amount of CHE remaining in the LNP fractions over 8 h. As expected, CHE is non-exchangeable and remains with the LNP over the 8 h time course for both particle sizes. (B) PEG-DMG dissociates at a rate of 26%/h from 80 nm diameter LNP and at a rate of 36%/h from 45 nm diameter LNP. (C) DSPC dissociates at a rate of 8%/h from 45 nm diameter LNP and 1%/h for 80 nm diameter systems. (D) DLin-MC3-DMA dissociates from 80 and 45 nm diameter LNP at 3%/h and 6%/h respectively. (E) 45 nm and 80 nm diameter LNP were formulated with siRNA conjugated to the Quasar 570 fluorophore, incubated with mouse plasma and separated by size exclusion. The amount that remained associated with LNP fractions was monitored for up to 16 h. Over 80% of the siRNA remained associated with the LNP fractions for at least 8 h. (F) LNP (30, 45 and 80 nm diameter) formulated with NBD and LRB–DOPE were incubated in plasma for up to 24 h. The NBD fluorescence intensity was measured as a readout of dissociation of DOPE from the LNP and normalized to the fluorescence intensity of samples incubated with 1.5% Triton X-100. The rates of dissociation were found to be correlated with particle size (dissociation rates for 80 nm diameter < 45 nm diameter < 30 nm diameter).

from 50 to 60 mol%, the activity of 30 nm LNP-siRNA systems was increased approximately three times from an ED_{50} of 0.8 mg/kg to <0.3 mg/kg (Fig. 4B). It is important to note that changes in particle size, amount of amino-lipid or amine-to-phosphate charge ratios do not result in changes in pKa (Supplementary Fig. 2) which is a critical parameter that dictates LNP-siRNA activity [9]. This strongly supports the proposal that the activity of smaller systems is compromised by the rapid dissociation of the amino-lipid component.

3.5. A PEG coating that dissociates slowly dramatically improves particle stability

PEG-lipids with longer carbon chains dissociate from LNP more slowly than those with shorter acyl chains [12,31]. Since the PEG-lipid comprises the coat lipid of the LNP [32] its loss would likely enhance the dissociation of other lipid components. In order to improve particle stability, PEG-DSG, which has alkyl chains of 18 carbons was used in

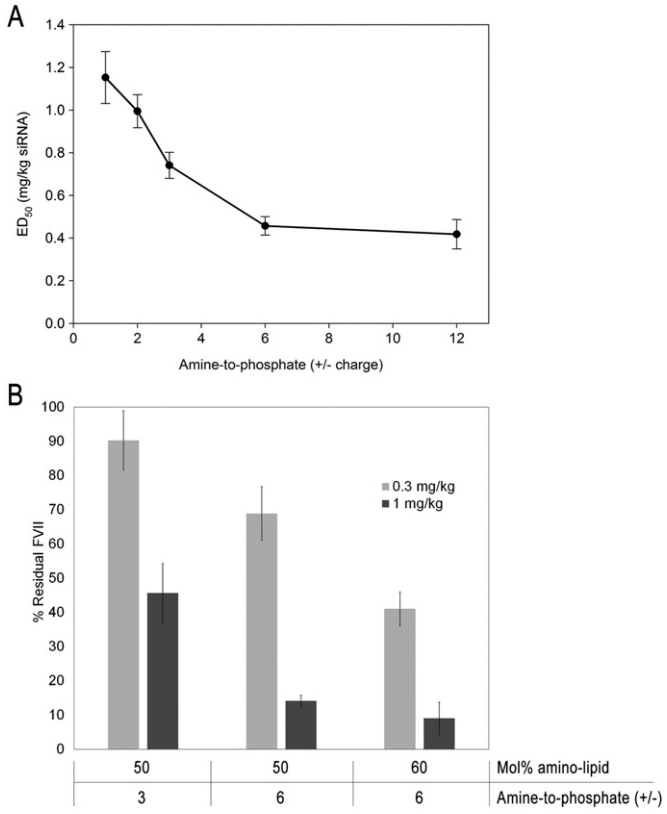

Fig. 4. The gene silencing potency of small LNP-siRNA systems can be improved by increasing the amount of amino-lipid in the LNP. (A) Small 30 nm diameter LNP-siFVII containing 50 mol% DMAP-BLP were formulated at amino-lipid-to-siRNA phosphate charge ratios of 1–12 and injected into mice at doses of 0.3, 1 and 3 mg siRNA/kg body weight. The ED_{50} for FVII gene silencing is plotted against the amine-to-phosphate charge ratios. $ED_{50} \pm$ s.e. are calculated from dose titration curves. (B) Small 30 nm diameter LNP-siRNA containing 50 mol% DMAP-BLP at an amine-to-phosphate ratio of 3 or 6 and 60 mol% DMAP-BLP at an amine-to-phosphate ratio of 6 were injected into mice at 0.3 and 1 mg/kg body weight. The residual FVII (%) is normalized to control mice. Results shown represent the mean ± s.d. of three animals.

place of PEG-DMG. Fig. 5 shows the dissociation rates of all lipid components in PEG-DSG LNP following incubation in mouse plasma. As expected, no measurable dissociation of the non-exchangeable ^{3}H-CHE was detected (Fig. 5A). PEG-DSG did dissociate from the LNP over time but at a significantly lower rate (24 and 47 h $t_{1/2}$ for 45 and 80 nm LNP) in comparison to PEG-DMG (1.1 and 1.7 h) (Fig. 5B). Similarly, the dissociation rate for DSPC was reduced with $t_{1/2}$ of 55 and 200 h for 45 and 80 nm LNP (Fig. 5C). Furthermore, as seen in Fig. 5D, DLin-MC3-DMA dissociation was also reduced (dissociation $t_{1/2}$ of 15 and 19 h). The siRNA cargo remained stably associated with the LNP fractions (> 90%) for up to 16 h regardless of the initial particle size (Fig. 5E).

3.6. The presence of PEG-DSG extends LNP-siRNA circulation lifetimes and reduces hepatic localization

A stable PEG coating on LNP systems results in long circulation lifetimes following i.v. administration and enhances distribution to disease sites such as tumour sites [33,34] and thus the LNP-siRNA systems containing PEG-DSG would be expected to exhibit different pharmacokinetics and biodistribution compared to systems containing PEG-DMG. Small, medium and large (~30, 45, 80 nm diameter) PEG-DSG LNP containing trace amounts of ^{3}H-CHE were formulated and blood levels assayed over 24 h in mice following i.v. administration. LNP containing PEG-DSG exhibited dramatically increased circulation lifetimes (Fig. 6A) compared to their counterparts containing PEG-DMG (Fig. 2A). The greatest difference is observed for 30 nm diameter PEG-DSG LNP, which has a circulation half-life of ~10.9 h compared to <0.25 h for PEG-DMG LNP of similar size. The 45 and 80 nm diameter PEG-DSG LNP have approximate circulation half-lives of 0.5 and 3 h, respectively. The relatively long circulation lifetime of 30 nm LNP can be attributed to the high PEG-lipid density on the surface which inhibits Apolipoprotein E (ApoE) adsorption and cellular accumulation [10,12].

Liver localization of LNP-siRNA was also affected by PEG-DSG. Not surprisingly, the rate of liver accumulation mirrors that of blood clearance (Fig. 6B). At 24 h post-injection, 70% of the total injected 45 nm LNP was found at the liver, whereas only 30% and 50% of the 30 nm and 80 nm LNP were found, respectively. Accumulation of LNP in the spleen, kidney, pancreas, lung, femurs and heart was also examined. Similar to the biodistribution profile of PEG-DMG LNP, less than 1% of the injected dose of any formulation was found in the pancreas, lung, femurs or heart (Fig. 6C). Interestingly, only 5% of the injected 80 nm PEG-DSG LNP accumulated in the spleen, compared to 10% for PEG-DMG LNP (Fig. 2C). Furthermore, there is an overall increase in the injected dose found in the kidney.

4. Discussion

Small LNP with diameters of 30 nm or less exhibit enhanced penetration into diseased tissues such as tumors following i.v. administration [19–21]. Similarly, we have recently shown that small LNP-siRNA are better able to reach regional lymph nodes and enter the circulation after being administered subcutaneously [15]. However, we show here that small LNP-siRNA systems that contain rapidly dissociating PEG-lipids are less potent than their larger counterparts, possibly because the amino-lipid component also rapidly dissociates from the smaller particles. This reduced potency can be partially rescued by increasing the mole fraction of amino-lipid in the LNP or by increasing the amine-to-phosphate charge ratio. Although these results relate to the liver, the overall activity of small LNP-siRNA likely translates to tissues that require deeper penetration such as in tumors. The mouse FVII gene silencing model used here represents a measure for LNP-siRNA activity [8,9,23,35]. The ability of LNP-siRNA to penetrate into tissues require other models such as 3D cell cultures or *in vivo* solid tumors which are currently being investigated in our laboratory. There are three aspects of this work that require discussion. The first concerns whether the time taken for the LNP-siRNA systems to reach the liver is long enough for appreciable loss of amino-lipid and second, whether factors other than amino-lipid content could be contributing to the poor potency of the smaller systems. The third topic concerns the delicate interplay between LNP size, amino-lipid content and the type of PEG-lipid employed and their effects on the biodistribution and gene silencing potency of LNP-siRNA systems. Methods for improving the potency of LNP systems with diameters less than 50 nm will also be addressed. We discuss these areas in turn.

In this work we have demonstrated a correlation between the reduced potency of small (~30 nm diameter) LNP-siRNA systems and the increased rate of dissociation of lipid components, particularly the amino-lipid, for the smaller systems (Fig. 3). The first question to be asked is whether there is adequate time following i.v. administration for the amino-lipid to dissociate to the extent that activity is compromised. It may be noted that the large majority of 30 and 45 nm diameter PEG-DMG LNP accumulate in the liver within 30 min post-injection (Fig. 2B), however lipid dissociation likely continues after extravasation into the space of Disse in the liver and during the early stages of endocytosis into hepatocytes. It was recently reported that siRNA-gold conjugates delivered by LNP systems were found in the hepatocyte cytosol 1.5–2 h post-administration [36]. As noted, the $t_{1/2}$ for amino-lipid in the 30 nm diameter LNP could not be measured directly however it can be extrapolated from the $t_{1/2}$ measured for the 45 and 80 nm diameter systems assuming that the proportion of lipid dissociating per unit time is proportional to the surface area/particle volume, or 1/radius. Under this assumption, and using the measured dissociation $t_{1/2}$ of

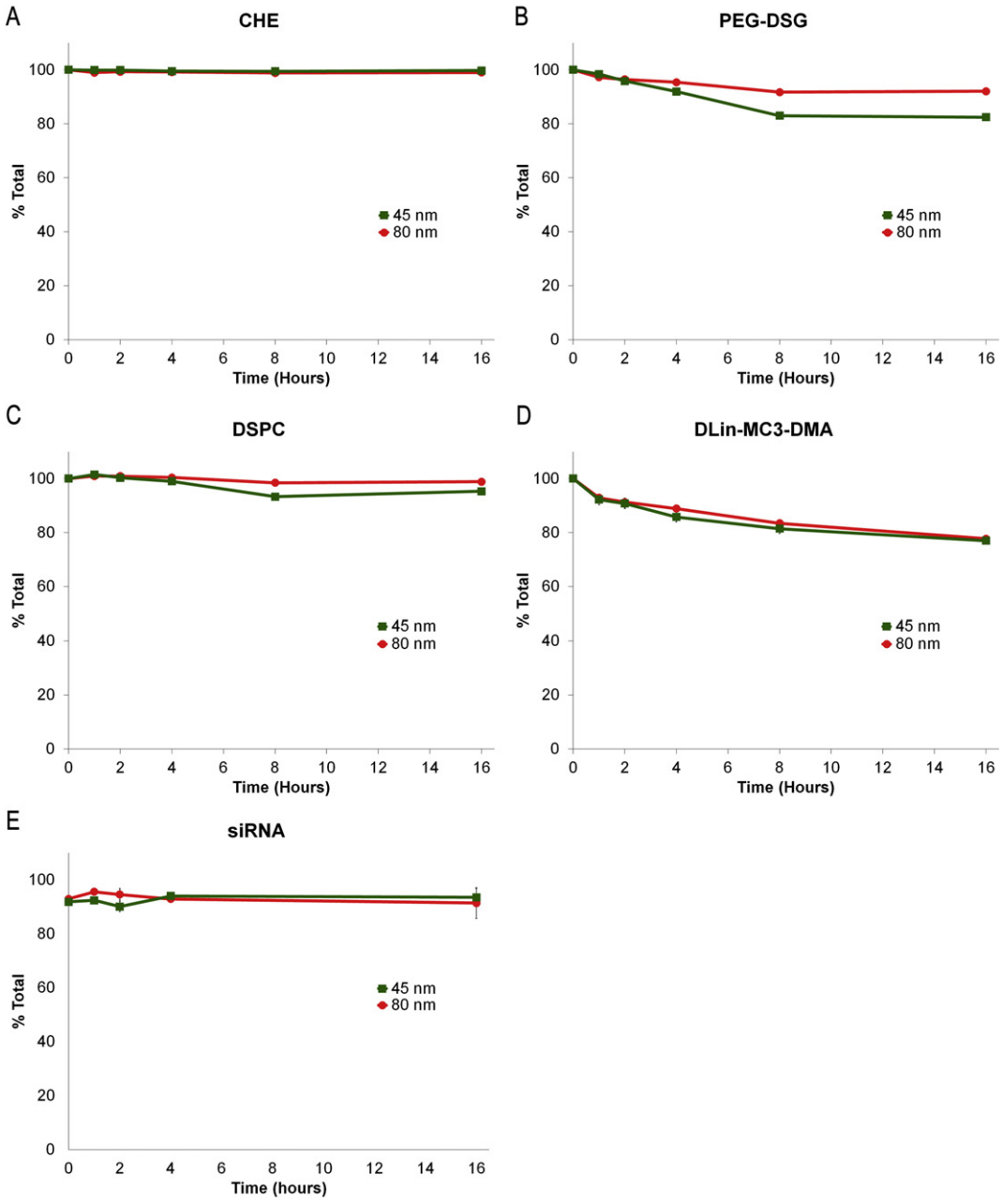

Fig. 5. Substitution of PEG-DMG for PEG-DSG greatly decreases the dissociation rates of component lipids. ^{3}H-PEG-DSG, ^{14}C-DSPC, ^{14}C-DLin-MC3-DMA or ^{3}H-CHE formulated with either 0.5 mol% or 1.5 mol% PEG-DSG were incubated for 0, 1, 2, 4, 8 and 16 h at 37 °C in mouse plasma and isolated by size exclusion chromatography. The rate of lipid dissociation from the LNP fractions was determined by using a linear fit for the first four time-points. (A) CHE remains associated with LNP. (B) PEG-DSG dissociates from 80 nm LNP at 1.2%/h and 2.2%/h for 45 nm LNP. (C) DSPC dissociates at less than 1%/h from both 80 and 45 nm diameter LNP. (D) DLin-MC3-DMA dissociates from 80 and 45 nm LNP at 2.6%/h and 3.3%/h respectively. (E) Over 90% of the siRNA remained associated with 45 and 80 nm diameter LNP for up to 16 h as assayed for siRNA conjugated to Quasar 570 fluorophore, incubated with mouse plasma and resolved by size exclusion.

DLin-MC3-DMA from 45 nm (4.9 h) and 80 nm diameter LNP (12 h) (Fig. 3D), the dissociation $t_{1/2}$ of DLin-MC3-DMA from 30 nm diameter LNP should be in the range of 3.9 h. Thus if it takes 2 h for the LNP to effectively deliver its cargo to the cell interior it can be estimated that the proportion of amino-lipid in the LNP would be reduced from 50 mol% to 46 mol% for 80 nm LNP, 40 mol% for 45 nm diameter LNP and 37 mol% for 30 nm LNP. As noted elsewhere pronounced reductions in LNP-siRNA gene silencing activity have been observed for >50 nm diameter LNP containing less than 50 mol% amino-lipid [8,9,14], consistent with the possibility that the limited activity of the 30 nm diameter systems arises at least in part from reduced levels of amino-lipid. It is important to note that despite being the most active LNP-siRNA, the 80 nm system had the lowest liver accumulation (~70% injected dose). Because the liver fenestrae are ~100 nm in diameter and 80 nm is the mean diameter of the size distribution, a small population of 80 nm LNP beyond 100 nm in diameter is likely excluded.

The second question is whether the reduction in potency of the smaller LNP-siRNA systems can be entirely attributed to enhanced lipid dissociation rates for smaller LNP. As shown in this work, a modest improvement in gene silencing potency was observed when the LNP amino-lipid-to-siRNA ratio was increased and a 3-fold improvement in potency was observed when the proportion of amino-lipid was increased to 60 mol% (Fig. 4B). Both these observations are consistent with loss of amino-lipid contributing to the reduced potency of the 30 nm systems. However even with increased overall proportions of amino-lipid, gene silencing activity cannot be raised to levels observed for the 80 nm

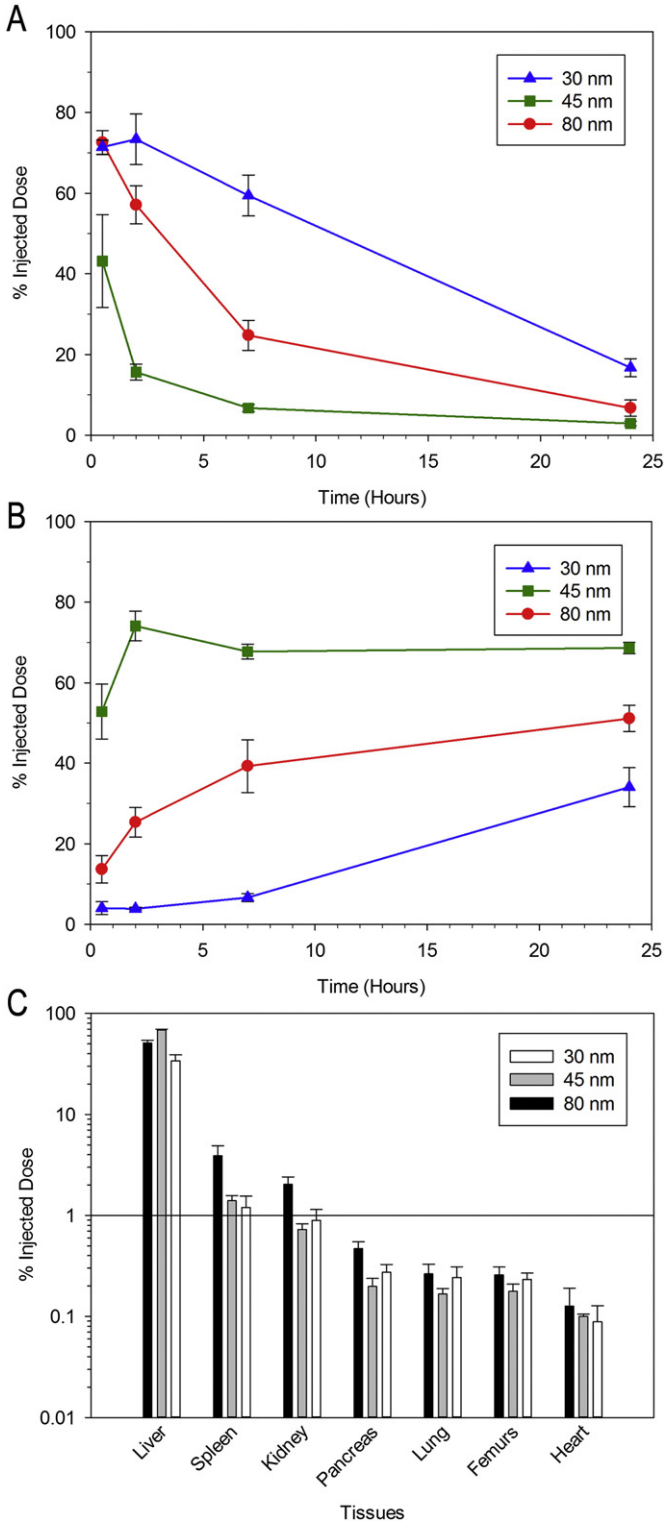

Fig. 6. Substitution of PEG-DMG for PEG-DSG results in increased LNP-siRNA circulation lifetimes. Small (30 nm), medium (45 nm) or large (80 nm) LNP formulated with PEG-DSG and labelled with trace amounts of ^{3}H-CHE were injected into mice at 0.3 mg siRNA/kg of body weight. Blood and tissues were collected at various time points and the amount of ^{3}H-CHE was determined. (A) Clearance of LNP from blood over a period of 24 h. (B) Accumulation of LNP in liver over 24 h. (C) Accumulation of LNP in various tissues at 24 h. Results shown represent the mean ± s.d. of four animals.

diameter systems (ED_{50} of 0.04 mg siRNA/kg *vs* ED_{50} of 0.3 mg siRNA/kg), suggesting that inefficient endosomal release resulting from diminished amino-lipid content cannot fully explain the overall reduction in potency of small LNP-siRNA systems. The difference in activity between large and small systems could arise due to differences in liver accumulation. However small and medium-sized (~30 and 45 nm diameter) PEG-DMG LNP exhibit similar clearance and liver accumulation kinetics (Fig. 2) yet have markedly different gene silencing potencies (Fig. 1). It is also conceivable that the higher initial PEG-lipid content for smaller LNP could have some influence on LNP-siRNA activity. Because particle size is directly related to the amount of PEG-lipid used, these variables are difficult to evaluate independently. Differential protein adsorption could also explain the difference in activity since it has been shown that the efficacy of LNP-siRNA requires the adsorption of ApoE [10]. LNP that differ in size also differs in surface curvature which could directly affect the type and amount of protein adsorbed. Another possibility is that the reduced activity of smaller systems is related to the reduced amino-lipid or siRNA payload for smaller LNP systems. For example, a 30 nm diameter LNP would only deliver ~1/20 as many siRNA copies as compared to an 80 nm diameter system.

The third topic for discussion concerns alternative ways of improving the gene silencing potency of small LNP-siRNA systems. We show here that the dissociation of lipid components from LNP can be dramatically reduced by utilizing the PEG-DSG coat lipid during formulation rather than the rapidly dissociating PEG-DMG lipid. However these systems are markedly less potent than systems containing PEG-DMG due to the long-lived PEG coat, which inhibits ApoE adsorption and prolongs circulation [10,12], illustrating the complex interplay between particle size, amino-lipid content and the type of PEG-lipid employed to achieve LNP-siRNA systems with high potencies *in vivo*. It is also interesting to note that in contrast to 30 nm LNP that contain PEG-DMG, those that contain PEG-DSG exhibit the longest circulation lifetimes. The reason for the long circulation lifetime for the smaller LNP can be attributed to the fact that this system contained 5 mol% PEG-DSG (which does not dissociate from the LNP). The reduced circulation lifetimes of the 45 nm diameter system can be attributed to the much lower PEG-DSG levels (1.5 mol%). The surprising observation that the 80 nm diameter system (which contained 0.5 mol% PEG-DSG) exhibits longer circulation lifetimes may arise due to reduced rates of liver accumulation as such systems will penetrate less readily through the fenestrated liver vasculature.

It is possible that further improvements in the potency of small (30 nm diameter) systems will only be achievable by new approaches. This is particularly true if the activity of smaller systems is fundamentally limited by the siRNA payload. It is possible to increase the amount of siRNA per particle by increasing the siRNA-to-lipid ratio to values approaching charge ratios of one, however >50 nm LNP-siRNA exhibit reduced gene silencing activity [14] which is consistent with our current findings for 30 nm systems (Fig. 4A), indicating excess cationic amino-lipid is necessary for endosomal release. It may be possible to improve the efficiency of siRNA release from endosomes following endocytosis, as it has been shown that only ~1–2% of endocytosed siRNA reaches the cytoplasm [36]. However methods for achieving this are not obvious. Replacement of DSPC with lipids such as DOPE may facilitate endosomal fusion somewhat [30,37]. If the limiting factor is the amount of amino-lipid per particle, it should be noted that incorporation of more than 60 mol% amino-lipid leads to progressively lower encapsulation efficiencies [38] and larger sizes and polydispersity (data not shown). Also, raising the amino-lipid content may compromise the therapeutic index of LNP-siRNA formulations as the dose limiting toxicity is related to the nanoparticle carrier [7,39].

In summary, we have shown that although LNP-siRNA systems with diameters <45 nm can be readily manufactured employing microfluidic mixing techniques, the gene silencing potency of these systems in hepatocytes *in vivo* is significantly reduced compared to their larger counterparts. At least part of this reduction in activity can be attributed to the reduced stability of smaller systems which leads to rapid dissociation of lipid components such as the amino-lipid. The activity of small LNP-siRNA can be improved by increasing the amino-lipid content which improves the potency by

approximately a factor of three, however these LNP systems are still approximately 10 times less potent than 80 nm diameter systems. It is possible that gene silencing potency of smaller systems is fundamentally limited by the small siRNA payload and that new approaches that enhance the efficiency of endosomal escape may be required for further gains in potency.

Acknowledgements

This work was supported by the Canadian Institutes for Health Research (CIHR FRN 111627), Alnylam Pharmaceuticals, and a Brain Canada Multi-Investigator Research Initiative Grant with matching support from Genome British Columbia, the Michael Smith Foundation for Health Research and the Koerner Foundation. We would like to thank Martin Maier and Akin Akinc at Alnylam Pharmaceuticals for their feedback, Alex Leung and Jayesh Kulkarni for helpful discussions, Yan Liu for technical assistance and Karen Lam for editing the manuscript.

Appendix A. Supplementary data

Supplementary data to this article can be found online at http://dx.doi.org/10.1016/j.jconrel.2016.05.059.

References

[1] A. de Fougerolles, H.P. Vornlocher, J. Maraganore, J. Lieberman, Interfering with disease: a progress report on siRNA-based therapeutics, Nat. Rev. Drug Discov. 6 (2007) 443–453.
[2] K.A. Whitehead, R. Langer, D.G. Anderson, Knocking down barriers: advances in siRNA delivery, Nat. Rev. Drug Discov. 8 (2009) 129–138.
[3] C.V. Pecot, G.A. Calin, R.L. Coleman, G. Lopez-Berestein, A.K. Sood, RNA interference in the clinic: challenges and future directions, Nat. Rev. Cancer 11 (2011) 59–67.
[4] A.K. Vaishnaw, J. Gollob, C. Gamba-Vitalo, R. Hutabarat, D. Sah, R. Meyers, T. de Fougerolles, J. Maraganore, A status report on RNAi therapeutics, Silence 1 (2010) 14.
[5] T.M. Allen, P.R. Cullis, Liposomal drug delivery systems: from concept to clinical applications, Adv. Drug Deliv. Rev. (2012).
[6] T. Coelho, D. Adams, A. Silva, P. Lozeron, P.N. Hawkins, T. Mant, J. Perez, J. Chiesa, S. Warrington, E. Tranter, M. Munisamy, R. Falzone, J. Harrop, J. Cehelsky, B.R. Bettencourt, M. Geissler, J.S. Butler, A. Sehgal, R.E. Meyers, Q. Chen, T. Borland, R.M. Hutabarat, V.A. Clausen, R. Alvarez, K. Fitzgerald, C. Gamba-Vitalo, S.V. Nochur, A.K. Vaishnaw, D.W. Sah, J.A. Gollob, O.B. Suhr, Safety and efficacy of RNAi therapy for transthyretin amyloidosis, N. Engl. J. Med. 369 (2013) 819–829.
[7] S.A. Barros, J.A. Gollob, Safety profile of RNAi nanomedicines, Adv. Drug Deliv. Rev. 64 (2012) 1730–1737.
[8] S.C. Semple, A. Akinc, J. Chen, A.P. Sandhu, B.L. Mui, C.K. Cho, D.W. Sah, D. Stebbing, E.J. Crosley, E. Yaworski, I.M. Hafez, J.R. Dorkin, J. Qin, K. Lam, K.G. Rajeev, K.F. Wong, L.B. Jeffs, L. Nechev, M.L. Eisenhardt, M. Jayaraman, M. Kazem, M.A. Maier, M. Srinivasulu, M.J. Weinstein, Q. Chen, R. Alvarez, S.A. Barros, S. De, S.K. Klimuk, T. Borland, V. Kosovrasti, W.L. Cantley, Y.K. Tam, M. Manoharan, M.A. Ciufolini, M.A. Tracy, A. de Fougerolles, I. MacLachlan, P.R. Cullis, T.D. Madden, M.J. Hope, Rational design of cationic lipids for siRNA delivery, Nat. Biotechnol. 28 (2010) 172–176.
[9] M. Jayaraman, S.M. Ansell, B.L. Mui, Y.K. Tam, J. Chen, X. Du, D. Butler, L. Eltepu, S. Matsuda, J.K. Narayanannair, K.G. Rajeev, I.M. Hafez, A. Akinc, M.A. Maier, M.A. Tracy, P.R. Cullis, T.D. Madden, M. Manoharan, M.J. Hope, Maximizing the potency of siRNA lipid nanoparticles for hepatic gene silencing in vivo, Angew. Chem. Int. Ed. Eng. 51 (2012) 8529–8533.
[10] A. Akinc, W. Querbes, S. De, J. Qin, M. Frank-Kamenetsky, K.N. Jayaprakash, M. Jayaraman, K.G. Rajeev, W.L. Cantley, J.R. Dorkin, J.S. Butler, L. Qin, T. Racie, A. Sprague, E. Fava, A. Zeigerer, M.J. Hope, M. Zerial, D.W. Sah, K. Fitzgerald, M.A. Tracy, M. Manoharan, V. Koteliansky, A. Fougerolles, M.A. Maier, Targeted delivery of RNAi therapeutics with endogenous and exogenous ligand-based mechanisms, Mol. Ther. 18 (2010) 1357–1364.
[11] L.Y. Song, Q.F. Ahkong, Q. Rong, Z. Wang, S. Ansell, M.J. Hope, B. Mui, Characterization of the inhibitory effect of PEG-lipid conjugates on the intracellular delivery of plasmid and antisense DNA mediated by cationic lipid liposomes, Biochim. Biophys. Acta 1558 (2002) 1–13.
[12] B.L. Mui, Y.K. Tam, M. Jayaraman, S.M. Ansell, X. Du, Y.Y. Tam, P.J. Lin, S. Chen, J.K. Narayanannair, K.G. Rajeev, M. Manoharan, A. Akinc, M.A. Maier, P. Cullis, T.D. Madden, M.J. Hope, Influence of polyethylene glycol lipid desorption rates on pharmacokinetics and pharmacodynamics of siRNA lipid nanoparticles, Mol. Ther.–Nucleic Acids 2 (2013) e139.
[13] I.V. Zhigaltsev, N. Belliveau, I. Hafez, A.K. Leung, J. Huft, C. Hansen, P.R. Cullis, Bottom-up design and synthesis of limit size lipid nanoparticle systems with aqueous and triglyceride cores using millisecond microfluidic mixing, Langmuir 28 (2012) 3633–3640.
[14] N.M. Belliveau, J. Huft, P.J. Lin, S. Chen, A.K. Leung, T.J. Leaver, A.W. Wild, J.B. Lee, R.J. Taylor, Y.K. Tam, C.L. Hansen, P.R. Cullis, Microfluidic synthesis of highly potent limit-size lipid nanoparticles for in vivo delivery of siRNA, Mol. Ther.–Nucleic Acids 1 (2012) e37.
[15] S. Chen, Y.Y. Tam, P.J. Lin, A.K. Leung, Y.K. Tam, P.R. Cullis, Development of lipid nanoparticle formulations of siRNA for hepatocyte gene silencing following subcutaneous administration, J. Control. Release 196C (2014) 106–112.
[16] H.S. Choi, Y. Ashitate, J.H. Lee, S.H. Kim, A. Matsui, N. Insin, M.G. Bawendi, M. Semmler-Behnke, J.V. Frangioni, A. Tsuda, Rapid translocation of nanoparticles from the lung airspaces to the body, Nat. Biotechnol. 28 (2010) 1300–1303.
[17] D.A. Rao, J.R. Robinson, Effect of size and surface properties of biodegradable PLGA-PMA: PLA:PEG nanoparticles on lymphatic uptake and retention in rats, J. Control. Release 132 (2008) e45–e47.
[18] T.M. Allen, C.B. Hansen, L.S. Guo, Subcutaneous administration of liposomes: a comparison with the intravenous and intraperitoneal routes of injection, Biochim. Biophys. Acta 1150 (1993) 9–16.
[19] S. Huo, H. Ma, K. Huang, J. Liu, T. Wei, S. Jin, J. Zhang, S. He, X.J. Liang, Superior penetration and retention behavior of 50 nm gold nanoparticles in tumors, Cancer Res. 73 (2013) 319–330.
[20] R.K. Jain, T. Stylianopoulos, Delivering nanomedicine to solid tumors, Nat. Rev. Clin. Oncol. 7 (2010) 653–664.
[21] H. Cabral, Y. Matsumoto, K. Mizuno, Q. Chen, M. Murakami, M. Kimura, Y. Terada, M.R. Kano, K. Miyazono, M. Uesaka, N. Nishiyama, K. Kataoka, Accumulation of sub-100 nm polymeric micelles in poorly permeable tumours depends on size, Nat. Nanotechnol. 6 (2011) 815–823.
[22] R.L. Rungta, H.B. Choi, P.J. Lin, R.W. Ko, D. Ashby, J. Nair, M. Manoharan, P.R. Cullis, B.A. Macvicar, Lipid nanoparticle delivery of siRNA to silence neuronal gene expression in the brain, Mol. Ther.–Nucleic Acids 2 (2013) e136.
[23] A. Akinc, A. Zumbuehl, M. Goldberg, E.S. Leshchiner, V. Busini, N. Hossain, S.A. Bacallado, D.N. Nguyen, J. Fuller, R. Alvarez, A. Borodovsky, T. Borland, R. Constien, A. de Fougerolles, J.R. Dorkin, K. Narayanannair Jayaprakash, M. Jayaraman, M. John, V. Koteliansky, M. Manoharan, L. Nechev, J. Qin, T. Racie, D. Raitcheva, K.G. Rajeev, D.W. Sah, J. Soutschek, I. Toudjarska, H.P. Vornlocher, T.S. Zimmermann, R. Langer, D.G. Anderson, A combinatorial library of lipid-like materials for delivery of RNAi therapeutics, Nat. Biotechnol. 26 (2008) 561–569.
[24] F. Braet, E. Wisse, Structural and functional aspects of liver sinusoidal endothelial cell fenestrae: a review, Comp. Hepatol. 1 (2002) 1.
[25] J. Snoeys, J. Lievens, E. Wisse, F. Jacobs, H. Duimel, D. Collen, P. Frederik, B. De Geest, Species differences in transgene DNA uptake in hepatocytes after adenoviral transfer correlate with the size of endothelial fenestrae, Gene Ther. 14 (2007) 604–612.
[26] Y. Stein, G. Halperin, O. Stein, Biological stability of [3H]cholesteryl oleyl ether in cultured fibroblasts and intact rat, FEBS Lett. 111 (1980) 104–106.
[27] S.C. Semple, T.O. Harasym, K.A. Clow, S.M. Ansell, S.K. Klimuk, M.J. Hope, Immunogenicity and rapid blood clearance of liposomes containing polyethylene glycol-lipid conjugates and nucleic acid, J. Pharmacol. Exp. Ther. 312 (2005) 1020–1026.
[28] G. Scherphof, J. Damen, J. Dijkstra, F. Roerdink, H. Spanjer, Interactions of liposomes with lipoproteins and liver cells in vivo and in vitro studies, in: G. Gregoriadis, G. Poste, J. Senior, A. Trouet (Eds.), Receptor-Mediated Targeting of Drugs, Springer, US 1984, pp. 267–295.
[29] M.J. Hope, M.B. Bally, L.D. Mayer, A.S. Janoff, P.R. Cullis, Generation of multilamellar and unilamellar phospholipid vesicles, Chem. Phys. Lipids 40 (1986) 89–107.
[30] I.M. Hafez, N. Maurer, P.R. Cullis, On the mechanism whereby cationic lipids promote intracellular delivery of polynucleic acids, Gene Ther. 8 (2001) 1188–1196.
[31] J.J. Wheeler, L. Palmer, M. Ossanlou, I. MacLachlan, R.W. Graham, Y.P. Zhang, M.J. Hope, P. Scherrer, P.R. Cullis, Stabilized plasmid-lipid particles: construction and characterization, Gene Ther. 6 (1999) 271–281.
[32] A.K. Leung, I.M. Hafez, S. Baoukina, N.M. Belliveau, I.V. Zhigaltsev, E. Afshinmanesh, D.P. Tieleman, C.L. Hansen, M.J. Hope, P.R. Cullis, Lipid nanoparticles containing siRNA synthesized by microfluidic mixing exhibit an electron-dense nanostructured core, J. Phys. Chem. C. Nanomater. Interfaces 116 (2012) 18440–18450.
[33] T.M. Allen, The use of glycolipids and hydrophilic polymers in avoiding rapid uptake of liposomes by the mononuclear phagocyte system, Adv. Drug Deliv. Rev. 13 (1994) 285–309.
[34] C. Allen, N. Dos Santos, R. Gallagher, G.N. Chiu, Y. Shu, W.M. Li, S.A. Johnstone, A.S. Janoff, L.D. Mayer, M.S. Webb, M.B. Bally, Controlling the physical behavior and biological performance of liposome formulations through use of surface grafted poly(-ethylene glycol), Biosci. Rep. 22 (2002) 225–250.
[35] K.T. Love, K.P. Mahon, C.G. Levins, K.A. Whitehead, W. Querbes, J.R. Dorkin, J. Qin, W. Cantley, L.L. Qin, T. Racie, M. Frank-Kamenetsky, K.N. Yip, R. Alvarez, D.W. Sah, A. de Fougerolles, K. Fitzgerald, V. Koteliansky, A. Akinc, R. Langer, D.G. Anderson, Lipid-like materials for low-dose, in vivo gene silencing, Proc. Natl. Acad. Sci. U. S. A. 107 (2010) 1864–1869.
[36] J. Gilleron, W. Querbes, A. Zeigerer, A. Borodovsky, G. Marsico, U. Schubert, K. Manygoats, S. Seifert, C. Andree, M. Stoter, H. Epstein-Barash, L. Zhang, V. Koteliansky, K. Fitzgerald, E. Fava, M. Bickle, Y. Kalaidzidis, A. Akinc, M. Maier, M. Zerial, Image-based analysis of lipid nanoparticle-mediated siRNA delivery, intracellular trafficking and endosomal escape, Nat. Biotechnol. 31 (2013) 638–646.
[37] H. Farhood, N. Serbina, L. Huang, The role of dioleoyl phosphatidylethanolamine in cationic liposome mediated gene transfer, Biochim. Biophys. Acta 1235 (1995) 289–295.
[38] A.K. Leung, Y.Y. Tam, S. Chen, I.M. Hafez, P.R. Cullis, Microfluidic mixing: a general method for encapsulating macromolecules in lipid nanoparticle systems, J. Phys. Chem. B 119 (2015) 8698–8706.
[39] A. Chonn, P.R. Cullis, D.V. Devine, The role of surface charge in the activation of the classical and alternative pathways of complement by liposomes, J. Immunol. 146 (1991) 4234–4241.